

The HARPS search for southern extrasolar planets^{★,★★}

XXV. Results from the metal-poor sample

N. C. Santos^{1,2,3}, M. Mayor³, X. Bonfils^{3,4}, X. Dumusque^{1,3}, F. Bouchy⁵, P. Figueira¹, C. Lovis³,
C. Melo⁶, F. Pepe³, D. Queloz³, D. Ségransan³, S. G. Sousa¹, and S. Udry³

¹ Centro de Astrofísica, Universidade do Porto, Rua das Estrelas, 4150-762 Porto, Portugal
e-mail: nuno@astro.up.pt

² Departamento de Física e Astronomia, Faculdade de Ciências, Universidade do Porto, Portugal

³ Observatoire de Genève, Université de Genève, 51 Ch. des Maillettes, 1290 Sauverny, Switzerland

⁴ Laboratoire d'Astrophysique, Observatoire de Grenoble, Université J. Fourier, CNRS (UMR 5571), BP 53,
38041 Grenoble Cedex 9, France

⁵ Institut d'Astrophysique de Paris, UMR 7095 CNRS, Université Pierre & Marie Curie, 98bis Bd Arago, 75014 Paris, France

⁶ European Southern Observatory, Casilla 19001, Santiago 19, Chile

Received 29 July 2010 / Accepted 12 October 2010

ABSTRACT

Searching for extrasolar planets around stars of different metallicity may provide strong constraints to the models of planet formation and evolution. In this paper we present the overall results of a HARPS (a high-precision spectrograph mostly dedicated to deriving precise radial velocities) program to search for planets orbiting a sample of 104 metal-poor stars (selected [Fe/H] below -0.5). Radial velocity time series of each star are presented and searched for signals using several statistical diagnostics. Stars with detected signals are presented, including 3 attributed to the presence of previously announced giant planets orbiting the stars HD 171028, HD 181720, and HD 190984. Several binary stars and at least one case of a coherent signal caused by activity-related phenomena are presented. One very promising new, possible giant planet orbiting the star HD 107094 is discussed, and the results are analyzed in light of the metallicity-giant planet correlation. We conclude that the frequency of giant planets orbiting metal-poor stars may be higher than previously thought, probably reflecting the higher precision of the HARPS survey. In the metallicity domain of our sample, we also find evidence that the frequency of planets is a steeply rising function of the stellar metal content, as found for higher metallicity stars.

Key words. techniques: radial velocities – techniques: spectroscopic – planets and satellites: formation – planetary systems – stars: abundances

1. Introduction

The past 15 years have seen a plethora of exoplanet discoveries, with more than 500 announcements so far¹. Mostly thanks to the development of the radial-velocity technique, some of the discovered planets have been found to have masses as low as ~ 2 times the mass of our Earth (Mayor et al. 2009). The holy grail of exoplanet searches, namely the first detection of an exo-Earth, is closer than ever.

The increasing number of detected planets is also providing strong constraints for the models of planet formation and evolution (Udry & Santos 2007; Ida & Lin 2004a; Mordasini et al. 2009a). Two main models of giant planet formation have been discussed in the literature. On the one hand, the core-accretion model tells us that giant planets can be formed by the accretion

of solids in a protoplanetary disk, building up a $\sim 10 M_{\oplus}$ core followed by rapid agglomeration of gas (Pollack et al. 1996; Ida & Lin 2004a; Mordasini et al. 2009a). On the other hand, the “disk instability” model suggests that giant planets may be the outcome of direct gravitational instability of the gas (Boss 1997; Mayer et al. 2002). The two models predict, however, very different outcomes for the planet formation process as a function of the chemical composition of the disk (i.e. density of solids) and stellar mass (Matsuo et al. 2007). In particular, while the core accretion model predicts a strong metallicity-planet correlation and a higher prevalence of giant planets around higher mass solar-type stars (Mordasini et al. 2009b; Laughlin et al. 2004), such trends are less evident for the disk instability process (Boss 2002, 2006).

Concerning stellar metallicity, the first large, uniform spectroscopic studies comparing large samples of stars with and without planets have confirmed former suspicions (Gonzalez 1997) that stars hosting giant planets are more metal-rich (on average) than single, field stars (Santos et al. 2001, 2004b; Fischer & Valenti 2005). Stellar mass is also suspected to have a strong influence on the planet formation process (Johnson et al. 2007; Lovis & Mayor 2007), but a clear understanding of this picture is required. This need has inspired the construction of

[★] Based on observations collected at the La Silla Parana Observatory, ESO (Chile) with the HARPS spectrograph at the 3.6-m telescope (ESO runs ID 72.C-0488, 082.C-0212, and 085.C-0063).

^{★★} Full Tables 1 and 3 are only available in electronic form at the CDS via anonymous ftp to

cdsarc.u-strasbg.fr (130.79.128.5) or via <http://cdsarc.u-strasbg.fr/viz-bin/qcat?J/A+A/526/A112>

¹ See updated table at <http://www.exoplanet.eu>.

specific samples to search for planets around stars of different mass/evolutionary states (e.g. Bonfils et al. 2005; Setiawan et al. 2005; Johnson et al. 2007; Lovis & Mayor 2007) and different chemical compositions (e.g. Tinney et al. 2003; Fischer et al. 2005; Da Silva et al. 2006; Santos et al. 2007; Sozzetti et al. 2009).

The HARPS guaranteed time observations (GTO) program started to follow several different samples of solar-type stars in October 2003 (Mayor et al. 2003). The unparalleled long-term precision of HARPS allowed discovery of several planets among the targets, including the large majority of the known planets with masses near the mass of Neptune or below (e.g. Santos et al. 2004a; Lovis et al. 2006; Mayor et al. 2009).

One of the HARPS GTO sub-samples was built to explore how frequently giant planets orbit metal-poor stars to determine the metallicity limit below which no giant planets can be observed. In this paper we present the overall results of this program. In Sects. 2 and 3 we present our initial sample and observations. In Sect. 4 we show how the sample was cleaned a posteriori of the presence of stellar binaries and fast-rotating, active stars. The orbital parameters for some of the binaries in the sample are also listed. The remaining stars are then discussed in Sect. 5. The three planets already announced and one more promising candidate are presented. We conclude in Sect. 6.

2. The HARPS metal-poor sample

To explore the low-metallicity tail of the planet-host stars' distribution, one of the samples studied within the HARPS GTO program followed 104 metal-poor or mild metal-poor solar-type stars. This sample was chosen based on a preliminary version of the large catalog of Nordström et al. (2004). From this catalog, we took all late-F, G, and K stars ($b - y > 0.330$) south of $+10^\circ$ of declination that have a visual V magnitude brighter than 12. From these, we then excluded all identified visual and spectroscopic binaries, all stars suspected to be giants, and all those with measured projected rotational velocity $v \sin i$ above $\sim 6.0 \text{ km s}^{-1}$ (to indirectly exclude the most active stars, for which it is not possible to achieve a high radial-velocity precision – Saar & Donahue 1997; Santos et al. 2000; Paulson et al. 2002). Finally, we considered only those targets with estimated photometric $[\text{Fe}/\text{H}]$ between -0.5 and -1.5 . As seen below, a detailed spectroscopic analysis has later shown that some of the targets fall significantly out of this metallicity interval (see Fig. 1).

The final 104 stars in the sample (Table 1) have their V magnitudes between 5.9 and 10.9, distributed around an average value of 8.7. After a 15-min exposure, these magnitudes allow us to obtain an S/N high enough to derive radial-velocities with a precision better than 1 m s^{-1} for the majority of the targets. We note, however, that not all of these were interesting targets for a high-precision radial velocity planet search program (Sect. 4).

Precise spectroscopic atmospheric parameters and masses for the targets were derived in a separate paper (Sousa et al. 2011). In Fig. 1 we plot the distributions of metallicities, temperatures, stellar masses, and V magnitudes for the sample. In the upper-left panel, the dashed line represents the whole sample, while the filled and dotted lines represent the distributions for stars with high amplitude long term radial velocity trends (discussed in Sect. 5.3.2) and stars with known planets (Sect. 5.3.1), respectively. Overall, the metallicity distribution peaks around -0.65 dex and has a strong fall above -0.4 dex. The sample includes, however, several stars with spectroscopic metallicity above ~ -0.5 dex, even though the initial cut, based on photometric metallicity estimates, was set at -0.5 dex. Some of these

outliers can be explained by the error bars, both in the spectroscopic and (initial) photometric metallicities (the sample had been cut using the latter). The most extreme cases (HD 62849, HD 123517, HD 144589, and CD-231087, all with $[\text{Fe}/\text{H}]$ above -0.3 dex) are less easy to explain, though. HD 62849 ($[\text{Fe}/\text{H}] = -0.17$) is a close visual binary (see Sect. 4.1). We cannot exclude light contamination from the secondary star having biased the derivation of the stellar parameters. In any case, this star was later excluded from the sample (Sect. 4). CD-2310879 is the hottest star in our sample, and it presents a high activity level (Sect. 5.3.3). We cannot reject that the presence of active regions has induced a systematic error in our parameters. No clear explanation exists for the remaining two stars, namely HD 123517 and HD 144589. Interestingly, both present clear long-term trends in the radial-velocity data (see discussion in Sect. 5.3.2). Their high metallicities may be a signature of long period giant planets.

The mass and effective temperature distributions are rather peaked, with maxima around $0.8 M_\odot$ and 5700 K . Both distributions are roughly Gaussian shaped, although the former shows a tail towards higher masses. All stars except HD 221580 (Sect. 4.2) have spectroscopic parameters (temperature and surface gravity) typical of dwarfs or subgiants (for more details see Sousa et al. 2011).

In Table 3, we present the basic stellar parameters for the sample stars, excluding objects discussed in Sect. 4. The effective temperatures, surface gravities, and stellar metallicities were taken from the detailed spectroscopic analysis presented in Sousa et al. (2011). The $B - V$ values were taken from the Hipparcos catalog (ESA 1997), when available, and for the remaining stars from the NOMAD catalog (Zacharias et al. 2004). The estimate of the projected rotational velocity $v \sin i$ was derived using a calibration based on the width of the HARPS cross-correlation function, similar to the one presented for CORALIE in Santos et al. (2002). Due to different observing uncertainties, we adopted a value of $< 1 \text{ km s}^{-1}$ for stars presenting an estimated $v \sin i$ below this value. The activity level of the star, denoted here by the S_{MW} and $\log R'_{\text{HK}}$ values², were derived from the analysis of the Ca II H and K lines in the HARPS spectra, using a methodology similar to the one presented in Santos et al. (2000).

3. Observations

From October 2003 to July 2010, a total of 1301 precise radial-velocity measurements were obtained with HARPS for the stars in our program. The observations were done as part of the HARPS GTO program, and later complemented by two separate follow-up programs for a few stars (ESO programs ID 082.C-0212 and 085.C-0063³) aimed at searching for Neptune-like planets orbiting a sample of moderately metal-poor stars. Most of the stars have 5 or more measurements (Fig. 2).

During the first three years of the survey, the measurements were obtained with $\sim 2 \text{ m s}^{-1}$ precision. The defined exposure times were not long enough to average out the “noise” coming from stellar oscillations (Bouchy et al. 2005). Since 2006, this strategy has been revised, and the full precision of HARPS was exploited. Exposure times were then set to be 900 s, allowing the precision of the individual measurements to be increased to below 1 m s^{-1} . The observing strategy used does not avoid other sources of noise, including those coming from stellar granulation

² Both are presented since the latter depends on $B - V$, a parameter that we do not control.

³ In this latter case only for a star discussed in Sect. 5.3.4.

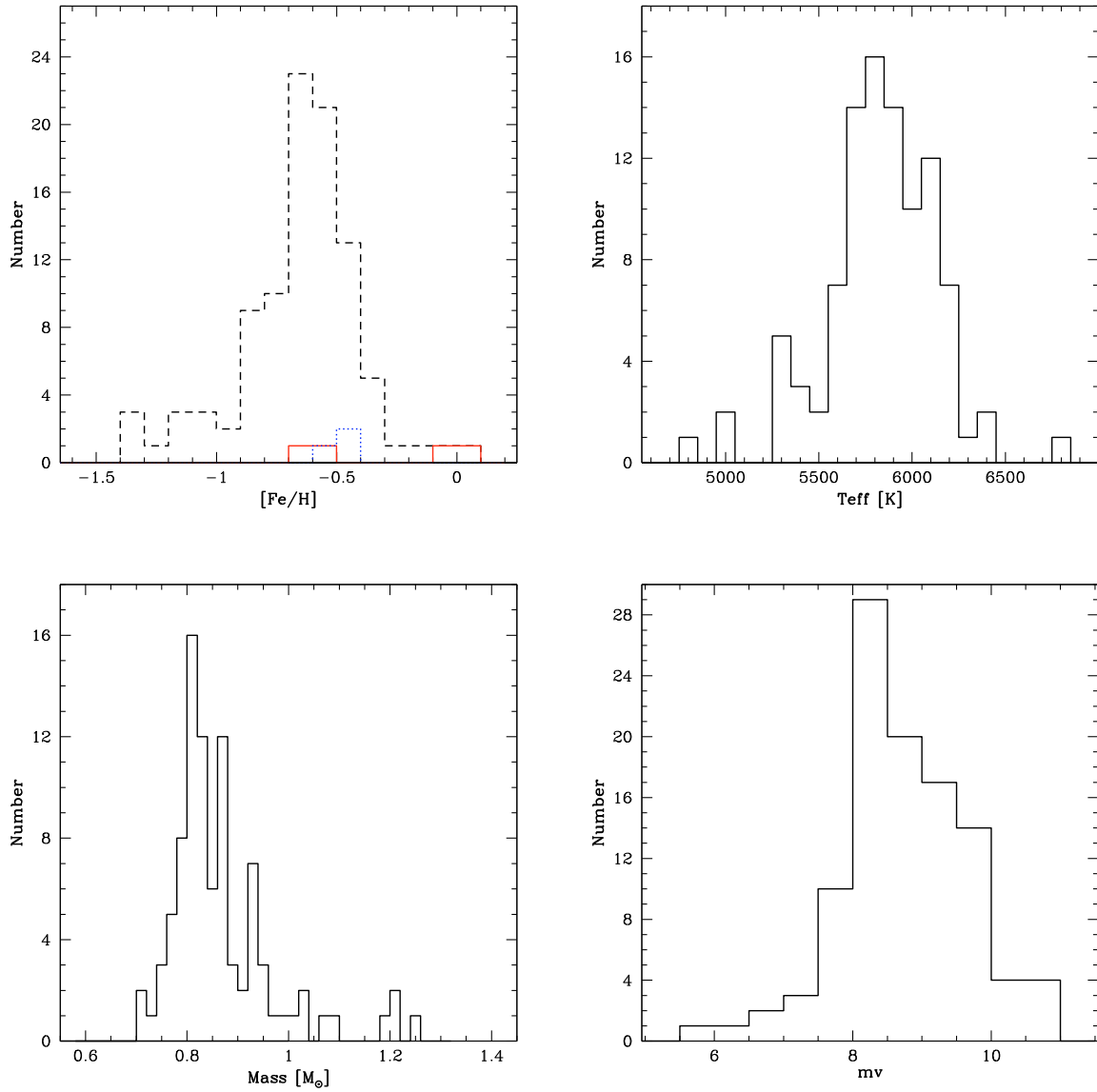


Fig. 1. Distributions of metallicity (*top left*), effective temperature (*top right*), stellar mass (*bottom left*), and visual magnitude (*bottom right*) for all the stars in our sample.

and activity (e.g. [Dumusque et al. 2011](#)). As seen in Fig. 2, if we consider only objects with at least 5 measurements, most of the stars present a radial-velocity rms of $\sim 1\text{--}2.5\text{ m s}^{-1}$, as expected. In this figure we limited the rms range to values up to $\sim 15\text{ m s}^{-1}$ for the sake of clarity. Only 10 objects fall above this limit.

The data were reduced using the latest version of the HARPS pipeline. This includes a correction for the secular acceleration (e.g. [Zechmeister et al. 2009](#)), for which we used Hipparcos parallaxes and proper motions ([ESA 1997](#)), whenever available.

4. Cleaning the sample

A few stars from our original sample were found to be unsuitable targets for a planet search survey for different reasons (binarity, activity, high rotation – Table 2). In this section we present these targets, which will be excluded from the rest of the discussion.

Table 1. List of targets, coordinates (equinox 2000.0), and magnitudes. Full table available in electronic form at the CDS.

Star	Alpha	Delta	m_v
HD 224817	00:00:58.2	−11:49:25	8.4
HD 967	00:14:04.4	−11:18:41	8.4
HD 11397	01:51:40.5	−16:19:03	9.0
HD 16784	02:40:38.7	−30:08:07	8.0
HD 17548	02:48:51.8	−01:30:34	8.2
...

4.1. Binaries

Though known binary stars were a priori excluded from the sample, a few SB1, SB2, or close visual binary systems passed through our first selection criteria. After a few measurements, these cases were usually discarded from the sample.

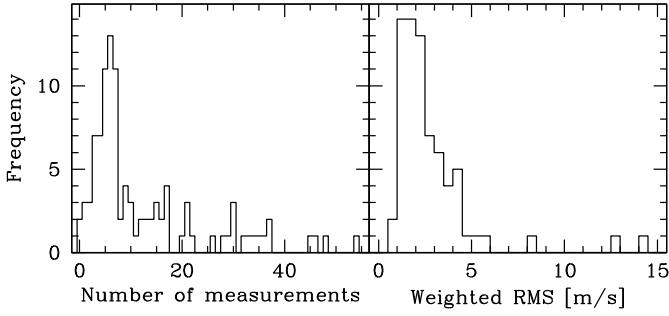


Fig. 2. *Left:* histogram of the number of radial-velocity measurements for the stars in our sample. *Right:* distribution of weighted rms values for our stars with at least 5 radial-velocity measurements. For clarity, the distribution is only shown for rms values below 15 m s^{-1} .

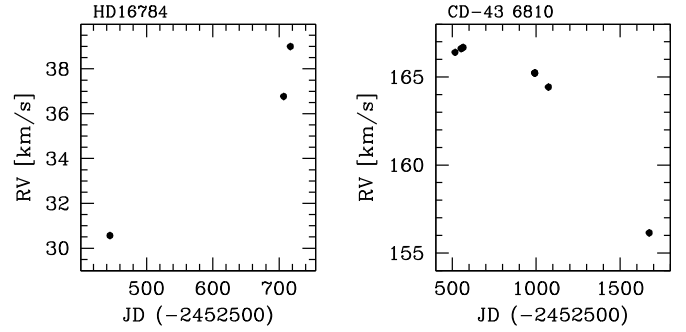


Fig. 3. Radial-velocity measurements of HD 16784 and CD-436810, two SB1 binaries from the sample.

Table 2. Stars excluded from the sample.

Star	Comment
BD-004234	Active/Fast rotator
BD-032525	SB2
CD-452997	SB1 [†]
CD-436810	SB1
HD 16784	SB1
HD 25704	Close visual binary
HD 62849	Close visual binary
HD 128575	Active/Fast rotator
HD 134113	SB1 [†]
HD 161265	SB2
HD 164500	SB2
HD 175179	Close visual binary
HD 187151	SB2
HD 197890	Active/Fast rotator
HD 221580	Giant
HD 224347	SB1 [†]

Notes. ^(†) Orbital fit was possible.

Three of these stars, HD 25704 (number of measurements, $N_{\text{mes}} = 20$), HD 62849 ($N_{\text{mes}} = 17$), and HD 175179 ($N_{\text{mes}} = 3$), were found to be close visual binary systems, after visual inspection of the guiding camera images. These have been at some point excluded from the sample given that the light contamination from the stellar companion in the HARPS fiber precludes any determination of precise radial velocities. This contamination is seeing dependent. These stars are not adequate for a planet search survey.

BD-032525 ($N_{\text{mes}} = 2$), HD 161265 ($N_{\text{mes}} = 2$), HD 164500 ($N_{\text{mes}} = 2$), and HD 187151 ($N_{\text{mes}} = 1$) were also excluded from the sample since an inspection of the cross-correlation function revealed that they are SB2 binaries. BD-032525 was also classified as a spectroscopic binary in Pourbaix et al. (2004) (after the beginning of our survey).

Five other stars in our sample were found to be SB1 binaries. For three of these (see next section), we obtained enough HARPS points to obtain a reliable orbital solution (Sect. 4.1.1). For the remaining two, HD 16784 ($N_{\text{mes}} = 3$; span=272 days) and CD-436810 ($N_{\text{mes}} = 9$; span=1157 days), the reduced number of measurements or their span did not allow us to fit any Keplerian function to the data (Fig. 3).

4.1.1. Binaries with orbital fits

For three of the binary stars in our sample, we gathered enough measurements to allow derivation of at least a tentative orbital solution.

HD 134113: though previously known to be a spectroscopic binary (Latham et al. 2002), we missed this classification when preparing the sample. A total of 28 precise radial-velocities were thus obtained for this star. A Keplerian fit to the data confirms and refines the previously suspected solution, with $P = 201.7$ days, $e = 0.89$, and $K = 3.9 \text{ km s}^{-1}$. The complete set of orbital parameters is listed in Table 4. Considering a stellar mass of 0.88 solar masses (Sousa et al. 2011), this signal is compatible with a minimum mass companion with 48 times the mass of Jupiter, a possible brown dwarf companion.

HD 224347: there is no previous reference in the literature of this star being a spectroscopic binary. Our 8 precise radial velocities obtained with HARPS show, however, a clear high-amplitude signal. The radial-velocities are well fit with a Keplerian function with period 6380 days, eccentricity of 0.56, and $K = 2.9 \text{ km s}^{-1}$. The large uncertainties (see Table 4) come from our data not covering one full orbital period, and the phase space is not covered well. This orbital solution should be considered as preliminary. Considering a stellar mass of 0.95 solar masses (Sousa et al. 2011), this signal is compatible with the presence of a minimum mass companion with 210 times the mass of Jupiter orbiting HD 224347.

CD-452997: 6 radial-velocity measurements of this star were obtained, showing a clear high-amplitude signal in the data. Though the number of measurements is small (and comparable with the number of free parameters to fit), a tentative Keplerian fit holds a period of 22.6 days, eccentricity of 0.50, and a semi-amplitude of 9.5 km s^{-1} . The signal is compatible with a 92 Jupiter mass stellar companion to this 0.72 solar mass star. We note, however, that this orbital solution should be regarded with caution.

4.2. Fast-rotating or giant stars

HD 221580: the 54 precise radial-velocity measurements of this star show a high-amplitude radial-velocity variation (total amplitude $\sim 80 \text{ m s}^{-1}$, $\text{rms} = 19.4 \text{ m s}^{-1}$). The data presents a rather complex behavior, and no clear periodicity could be found. Later detailed spectroscopic analysis has revealed that this star is a metal-poor giant, with $T_{\text{eff}} = 5322 \text{ K}$, $\log g = 2.68$, and $[\text{Fe}/\text{H}] = -1.13$ (Sousa et al. 2011). The observed “noise” is thus likely to be related to intrinsic stellar variability. Very similar stellar parameters were derived by Gratton et al. (2000), who

Table 3. List of targets with number of measurements, time span between first and last measurements, average radial velocity, stellar atmospheric parameters, $B - V$ color, activity level, and $v \sin i$. Full table available in electronic form at the CDS.

Star	N	Span [days]	$\langle RV \rangle$ [km s ⁻¹]	T_{eff} [K]	$\log g$ [cgs]	[Fe/H]	S_{MW}	$\sigma(S_{\text{MW}})$	$B - V$	$\log R'_{\text{HK}}$	$v \sin i$ [km s ⁻¹]
HD 967	34	2132	-24.3	5568 ± 17	4.53 ± 0.02	-0.68 ± 0.01	0.176	0.003	0.645	-4.91	<1
HD 11397	33	2075	41.1	5564 ± 26	4.46 ± 0.04	-0.54 ± 0.02	0.184	0.002	0.693	-4.89	<1
HD 17548	10	1504	-15.4	6011 ± 26	4.44 ± 0.02	-0.53 ± 0.02	0.162	0.005	0.529	-4.91	<1
HD 17865	21	1853	31.9	5877 ± 24	4.32 ± 0.03	-0.57 ± 0.02	0.159	0.002	0.568	-4.96	<1
HD 22879	36	1857	120.4	5884 ± 33	4.52 ± 0.03	-0.81 ± 0.02	0.165	0.003	0.554	-4.91	<1
...

Table 4. Elements of the fitted orbits for SB1 binaries.

	HD 134113	HD 224347	CD-45 2997 [†]	
P	201.674 ± 0.008	6380 ± 2500	22.6	[d]
T	2 453 984.87 ± 0.01	2 453 665 ± 78	2 453 176.8	[d]
a	0.66	7.0	0.15	[AU]
e	0.888 ± 0.001	0.56 ± 0.11	0.50	
V_r	-60.19 ± 0.06	1.38 ± 0.17	39.2	[km s ⁻¹]
ω	163.1 ± 0.2	221 ± 4	172	[deg]
K_1	3907 ± 42	2890 ± 210	9500	[m s ⁻¹]
$f_1(m)$	121 138 × 10 ⁻⁶	9062.746 × 10 ⁻⁶	1301.588 × 10 ⁻⁶	[M_{\odot}]
$\sigma(\text{O-C})$	1.55	0.56	–	[m s ⁻¹]
N	28	8	6	
$m_2 \sin i$	48	210	92	[M_{Jup}]

Notes. ^(†) Number of points is similar to number of free parameters; no errors available.

classified this star as a red horizontal branch giant. No reference to its evolutionary status is given in Nordström et al. (2004).

HD 128575, *HD 197890*, and *BD-00 4234*: these three stars were excluded from the sample since the first (and only) obtained HARPS spectrum has shown that their CCFs were very large and shallow, or were very difficult to identify. This behavior is typical of fast-rotating stars. These objects are not suitable for a precise radial velocity search for planets.

5. Results

After removing the 16 targets discussed above, we are left with 88 stars that we consider suitable for a high-precision radial-velocity planet search. From these, however, 24 objects have 5 or less measurements, making it difficult to make any firm conclusions. These are discussed separately from the others. For the remaining 64 stars (with 6 or more measurements), a more detailed analysis is done.

5.1. Stars with ≤5 measurements

Besides several of the cases discussed in Sect. 4, 24 stars in our sample were observed only 5 or less times during the period of our survey (Table 5, Fig. 5; one star, with one single measurement, was not included in the figure). With so few measurements, not much information can be extracted about these targets: a Keplerian fit, for instance, has 6 free parameters. We thus decided to separate all the targets with this reduced number of observations from the rest of the sample.

In Table 5 we present the list of targets in such conditions, their weighted average radial velocity, the weighted rms of the measurements, the average error of the obtained radial velocities, the number of measurements, as well as their time span. A look at the dispersions and average values shows that none of these

stars seems to present strong radial-velocity variations. All dispersions are below 5 m s⁻¹. Though the measurement time sampling may hide important signals, we can confidently exclude the existence of giant planets in short-period orbits around these stars. A statistical approach to this issue will be taken in a separate paper.

5.2. Tests for stars with at least 6 measurements

For stars with 6 or more radial-velocity measurements (64 objects – Fig. 6), we performed a series of statistical tests, following the same methodology applied to the HARPS M-dwarf sample (Bonfils et al. 2010). First, to test whether the observed RVs (σ_e) are significantly in excess of the internal errors (σ_i), we performed an F -test and derived the probability, $P(F)$, to the F -value $F = \frac{\sigma_e^2}{\langle \sigma_i^2 \rangle}$ (see e.g. Zechmeister et al. 2009). We also computed the χ^2_{constant} for the constant model as well as the probability of having χ^2_{constant} given the σ_i , $P(\chi^2_{\text{constant}})$. These values are listed in Tables 6 and 7. For 16 out of the 64 stars, both $P(F)$ and $P(\chi^2_{\text{constant}})$ are below 1%. These are the cases of CD-2310879, HD 11397, HD 59984, HD 88725, HD 107094, HD 109310, HD 123517, HD 124785, HD 144589, HD 150177, HD 171028, HD 171587, HD 181720, HD 190984, HD 215257, and HD 224817.

We note that the internal errors include both photon noise errors and errors from the wavelength calibration and instrumental drift correction. Furthermore, we added an instrumental error of 0.8 m s⁻¹ to take the estimated intrinsic precision of HARPS (guiding and internal errors) into account. Other sources of noise, like those coming from stellar intrinsic phenomena, are more difficult to estimate, so were not considered here.

Two tests were also done to estimate the probability that the observed radial velocities are best fitted by a linear function of type $rv = a \times \text{time} + b$. First, we used an F -test to derive the

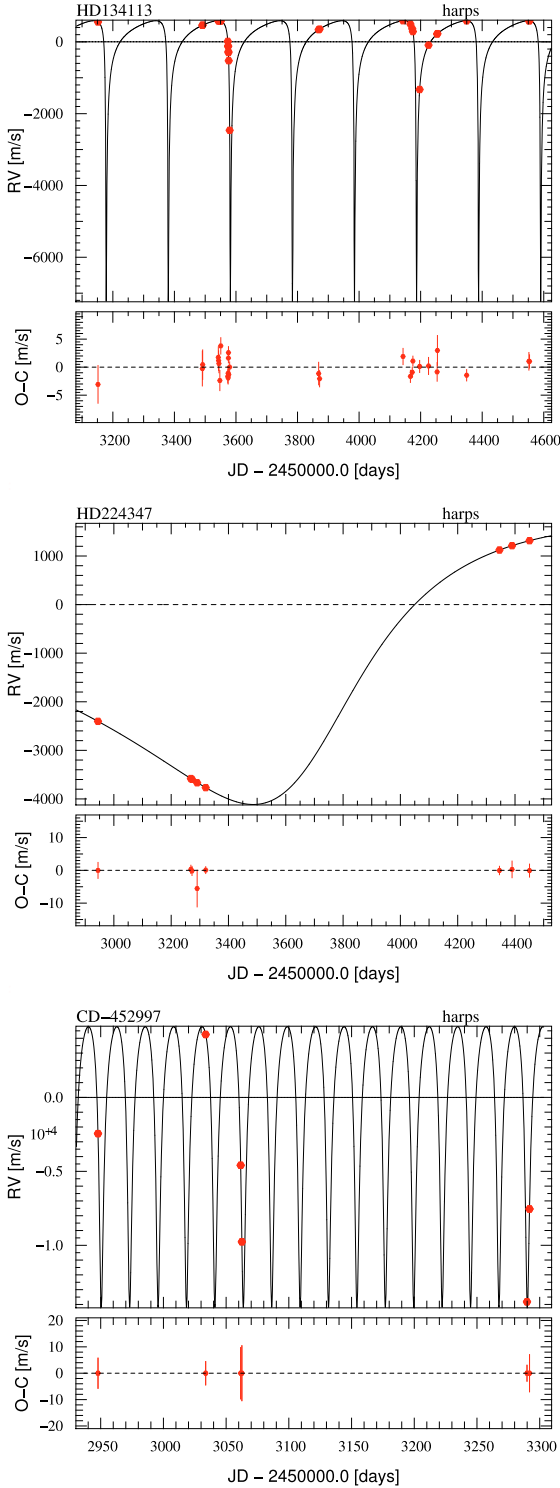


Fig. 4. *Top:* radial-velocity measurements of HD 134113 as a function of time, and the best Keplerian fit to the data. The residuals of the fit are shown in the *lower panel*. *Center and bottom:* same for HD 224347 and CD-452997, respectively.

probability $P(F_{\text{slope}})$ that the use of an additional free parameter (2 instead of 1 in case of a constant fit) implies a statistically significant improvement when comparing χ^2_{slope} to χ^2_{constant} . Second, we derived the false alarm probability using a bootstrap randomization approach. In this case, we generated random RV time series by shuffling (without repetition)

Table 5. Stars with 5 or less measurements.

Star	$\langle RV \rangle^\dagger$ [km s ⁻¹]	$\sigma(RV)^\dagger$ [m s ⁻¹]	$\langle \sigma_{\text{mes}} \rangle$ [m s ⁻¹]	N	Span [days]
BD-084501	84.469	1.7	7.4	3	1077
BD+062932	-144.809	1.0	2.2	4	1036
BD+063077	46.843	—	7.3	1	—
BD+083095	-51.148	3.2	3.3	3	1378
CD-4512460	108.847	3.8	6.3	4	1001
HD 38510	183.828	2.6	2.8	5	1502
HD 105004	121.495	3.9	3.1	5	1084
HD 111515	2.657	0.9	2.0	5	1458
HD 119949	-39.327	2.6	3.0	5	1463
HD 121004	245.318	1.7	2.0	5	1470
HD 128340	2.997	2.0	2.7	5	1031
HD 129229	-15.932	1.9	2.0	5	1031
HD 131653	-67.090	1.7	1.2	4	1375
HD 134088	-61.111	1.0	1.3	4	1377
HD 145344	-11.875	1.8	3.6	5	1378
HD 145417	8.799	1.3	2.2	5	1378
HD 147518	-42.127	0.6	2.0	4	1373
HD 193901	-171.416	2.2	2.8	3	1371
HD 195633	-45.832	3.1	3.0	4	346
HD 196892	-34.498	4.1	2.5	3	602
HD 197536	-17.117	1.4	2.0	3	1286
HD 199289	-6.144	1.2	2.6	5	1123
HD 207190	-11.314	1.3	2.5	5	1365
HD 223854	19.596	2.4	1.8	4	1401

Notes. ^(†) Weighted values.

the original radial velocity data, preserving the same observing dates. On each obtained time series, we adjusted a slope and computed its χ^2 value. The fraction of simulated data sets with χ^2 lower than the observed one gives us the false-alarm probability (FAP) for the slope model. Thirteen (13) stars in our sample show both significant $P(F_{\text{slope}})$ and FAP values: HD 11397, HD 56274, HD 77110, HD 79601, HD 88725, HD 107094, HD 109310, HD 113679, HD 123517, HD 144589, HD 148211, HD 190984, and HD 215257.

For stars with at least 12 measurements (37 stars), a test was also done to search for previously undetected periodic signals in the data. For this we analyzed the generalized lomb scargle periodogram. We followed the prescription used in Bonfils et al. (2010), Cumming et al. (1999), and Zechmeister & Kürster (2009). In brief, we created 10 000 virtual time series by making permutations of the original radial velocity set. For each case we then computed a periodogram and located the highest power. We then derived the distribution of the power maxima. We finally attributed an FAP to the maximum power value found in the original data set by counting the fraction of the simulated power maxima that have a higher value. The resulting FAP values are listed in Table 8, together with the amplitude of the period and amplitude of the highest peak in the periodogram of the real data. For stars with known planetary companions, both FAP before and after the subtraction of the Keplerian solution are shown, while for stars presenting linear drifts the test was done only after the subtraction of the trend. This was done since a linear drift will introduce extra power at low frequencies, masking any shorter period significant peaks. Six (6) stars in our sample show the presence of significant peaks (FAP below or near 1%): CD-2310879, HD 78747, HD 107094, HD 171028, HD 181720, and HD 190984.

Finally, for all the targets a Keplerian analysis was done using *yorbit* (Ségransan et al., in prep.), a code that uses an hybrid method based on a fast linear algorithm (Levenberg-Marquardt)

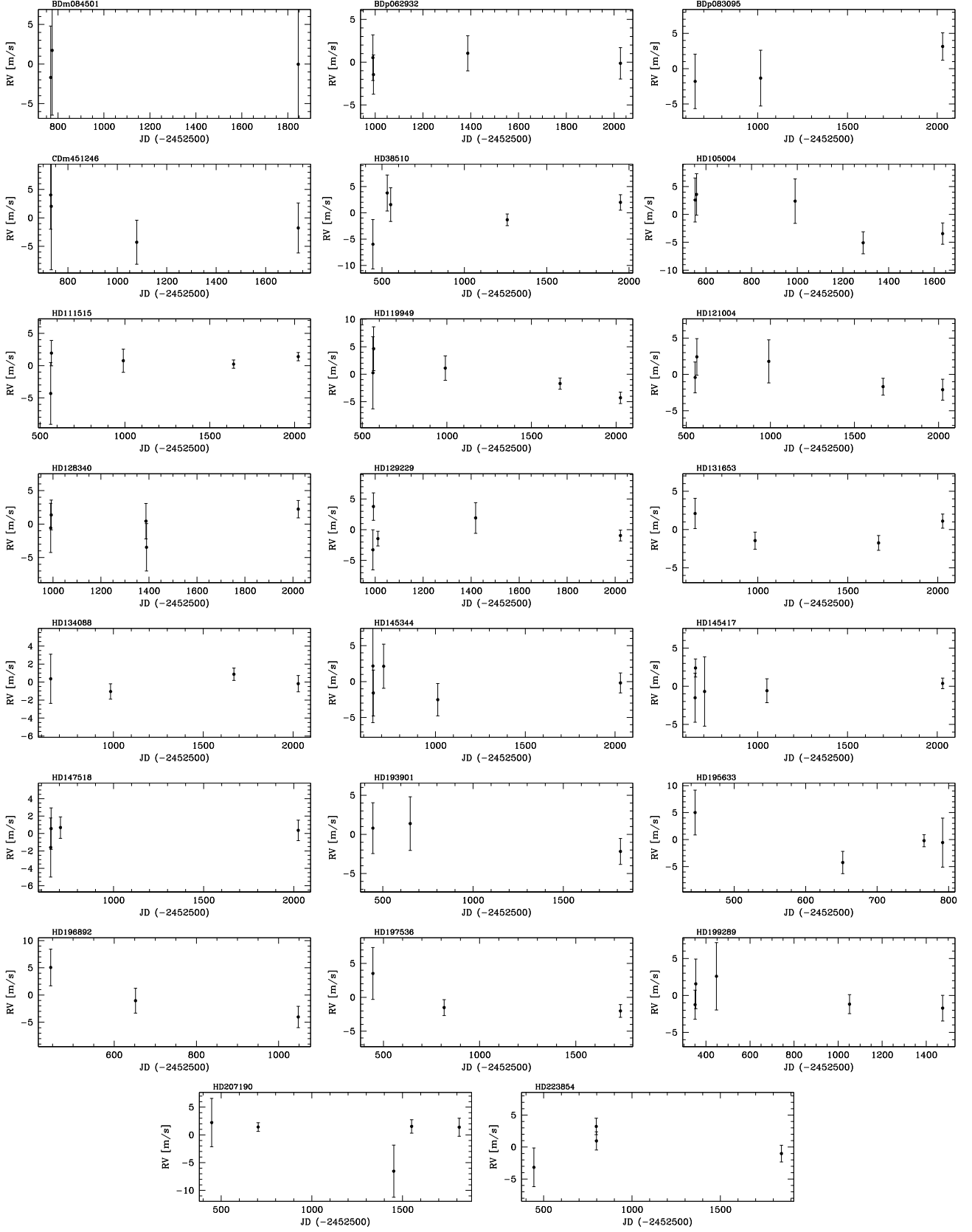


Fig. 5. Radial velocity time series for stars with 2 to 5 radial velocity measurements.

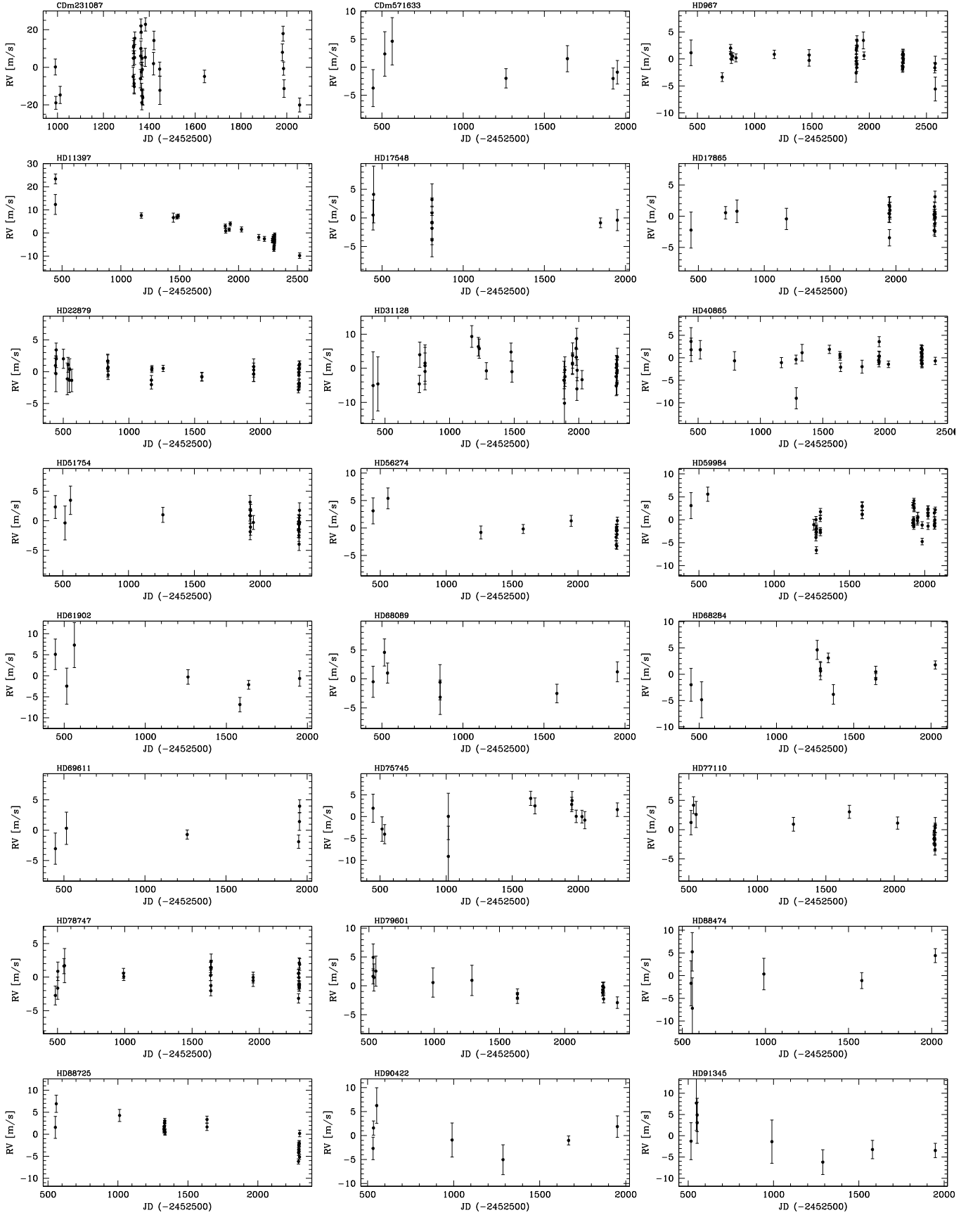


Fig. 6. Radial velocity time series for stars with at least 6 radial velocity measurements.

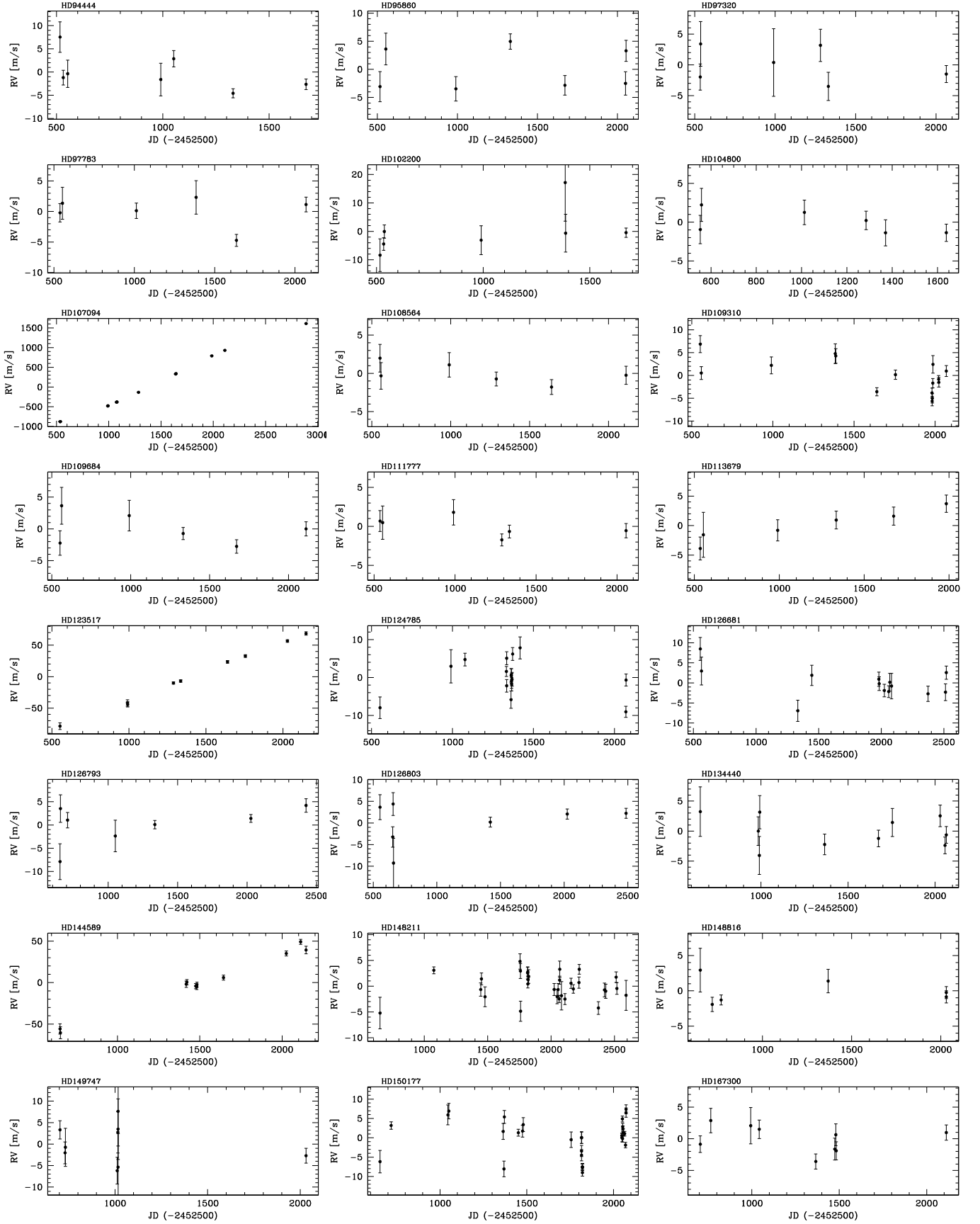


Fig. 6. continued.

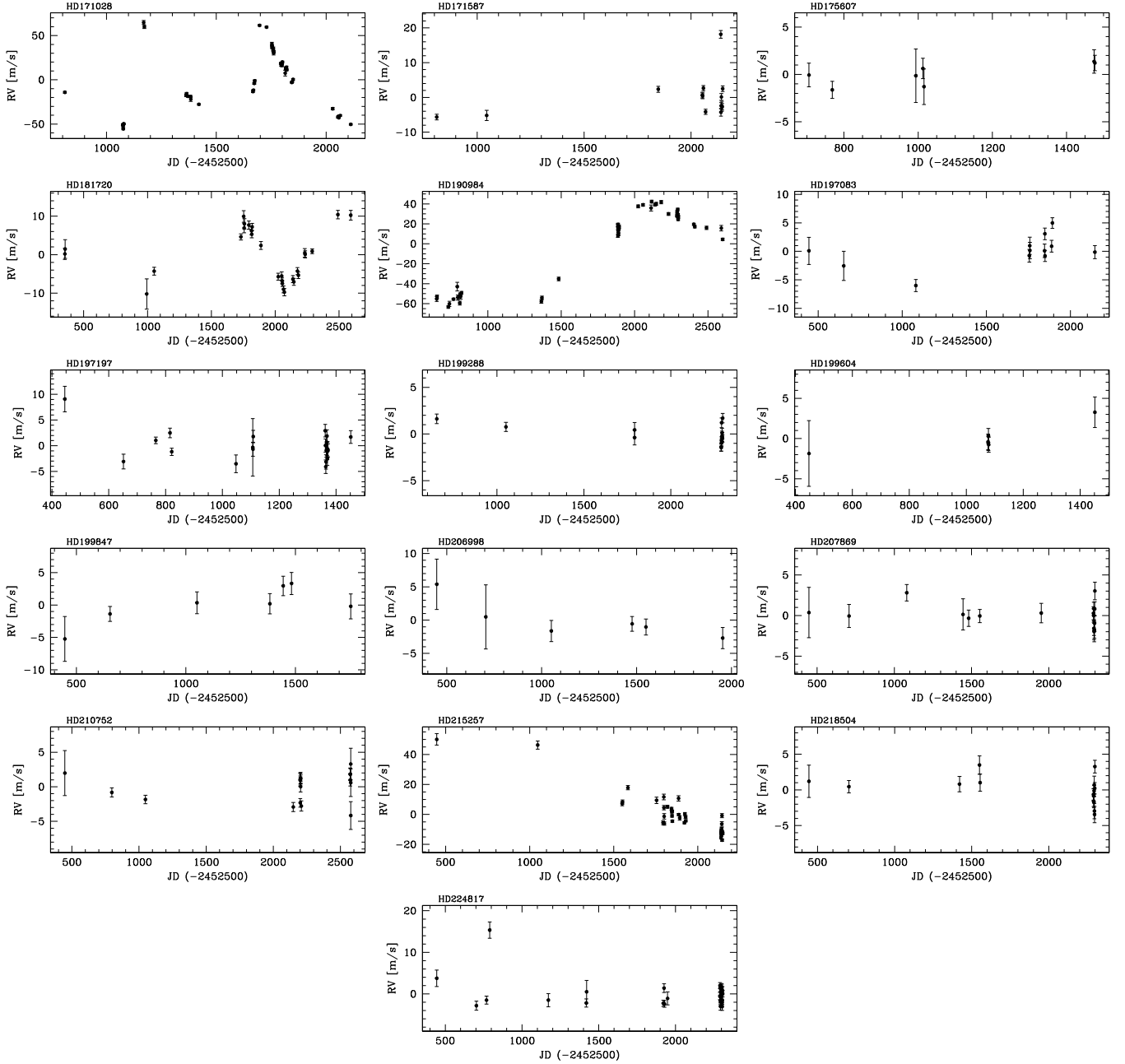


Fig. 6. continued.

and genetic operators (breeding, mutations, cross-over). This approach is important since in a periodogram an eccentric orbit is translated into not one but multiple peaks, making it difficult to identify the correct orbital parameters.

5.3. Case-by-case analysis

For 9 of the cases mentioned above, HD 11397, HD 123517, HD 144589, and HD 215257 (clear linear drifts), HD 171028, HD 181720, and HD 190984 (previously announced planets), CD-2310879 (active star), and HD 107094 (candidate new planet), the cause of the observed variation will be discussed in Sects. 5.3.1, 5.3.2, 5.3.3, and 5.3.4. A discussion of the remaining stars presenting some sort of variability according to the statistical tests is done below.

HD 56274 ($N_{\text{mes}} = 14$): the radial velocities of this star suggest the existence of a very low-amplitude drift (~ -0.8 m/s/yr), and our data does not allow us to reach any firm conclusions. No other significant signal is found in the data. No planet has been detected around this star by other high-precision radial velocity surveys (e.g. Fischer & Valenti 2005).

HD 59984 ($N_{\text{mes}} = 45$): this star shows an rms that is clearly above the average photon noise error. A period search (using both a periodogram and a Keplerian analysis) did not find any significant periodic signal in the data. The high dispersion observed may likely be explained by the evolutionary status of the star. Indeed, Sousa et al. (2011) derive a surface gravity of 4.18 dex for this $T_{\text{eff}} = 5962$ K metal-poor star ($[\text{Fe}/\text{H}] = -0.69$), indicating that it may be slightly evolved out of the main sequence. Evolved stars are known to have higher oscillation and

Table 6. Variability tests for stars with at least 6 measurements (CD and HD numbers up to 100 000).

Name	<i>N</i>	σ_i [m s ⁻¹]	σ_e [m s ⁻¹]	$P(F)$	χ^2_{constant}	$P(\chi^2_{\text{constant}})$	Slope [m/s/yr]	χ^2_{slope}	$P(F_{\text{slope}})$	FAP
CD-2310879	35	4.2	12.4	<10⁻⁹	336	<10⁻⁹	0.476	336	1.000	0.961
CD-571633	7	2.9	2.9	0.645	5.3	0.505	-0.244	4.5	0.686	0.107
HD 967	34	1.3	1.8	0.028	56.9	0.006	-0.154	55.4	0.674	0.009
HD 11397	33	1.4	6.3	<10⁻⁹	462	<10⁻⁹	-4.579	50.1	<10⁻⁹	<1/720
HD 17548	10	2.8	2.3	0.823	4.8	0.851	-0.244	4.2	0.496	0.028
HD 17865	21	1.5	1.6	0.450	27.4	0.123	-0.073	27.3	1.000	0.548
HD 22879	36	1.3	1.4	0.468	49.0	0.059	-0.297	40.4	<10⁻⁹	0.077
HD 31128	37	3.7	4.3	0.245	57.5	0.013	-0.547	54.5	0.035	0.070
HD 40865	30	1.5	2.3	0.014	48.3	0.014	0.062	48.1	1.000	0.019
HD 51754	21	1.6	1.9	0.333	29.8	0.072	-0.729	22.4	1.3 × 10⁻⁴	0.016
HD 56274	14	1.3	2.3	0.035	35.8	6.3 × 10⁻⁴	-0.783	23.4	0.002	0.002
HD 59984	45	1.2	2.4	2.0 × 10⁻⁶	202	<10⁻⁹	0.712	185	6.0 × 10⁻⁶	0.019
HD 61902	7	2.9	4.8	0.217	20.0	0.003	-1.362	11.1	0.106	0.056
HD 68089	7	2.4	2.6	0.598	7.2	0.302	-0.412	6.6	0.902	0.586
HD 68284	10	1.9	3.0	0.167	21.4	0.011	0.459	17.6	0.305	0.026
HD 69611	6	1.8	2.5	0.392	13.4	0.020	0.774	10.4	0.609	0.365
HD 75745	13	2.8	3.6	0.252	18.9	0.092	0.722	12.9	0.008	0.023
HD 77110	16	1.4	2.1	0.089	35.5	0.002	-0.964	15.9	2.0 × 10⁻⁶	<1/720
HD 78747	26	1.2	1.6	0.184	40.5	0.026	-0.137	39.3	0.799	0.099
HD 79601	16	1.6	2.0	0.282	23.6	0.071	-0.569	11.2	4.0 × 10⁻⁶	<1/720
HD 88474	6	3.9	4.5	0.534	9.6	0.088	1.035	5.9	0.274	0.177
HD 88725	22	1.2	3.3	1.3 × 10⁻⁵	179	<10⁻⁹	-1.879	46.8	<10⁻⁹	<1/720
HD 90422	7	2.6	3.6	0.347	8.6	0.199	-0.318	8.1	0.970	0.159
HD 91345	8	4.0	4.7	0.476	13.1	0.070	-1.574	4.8	0.006	0.021
HD 94444	7	2.3	4.0	0.181	24.8	3.7 × 10⁻⁴	-1.413	13.7	0.101	0.162
HD 95860	7	2.3	3.7	0.204	20.8	0.002	0.059	20.3	0.997	0.900
HD 97320	6	3.1	2.8	0.726	5.9	0.318	-0.283	4.9	0.741	0.471
HD 97783	6	1.9	2.5	0.443	15.3	0.009	-0.300	13.2	0.816	0.748

granulation noise (e.g. Mayor et al. 2003; Christensen-Dalsgaard 2004; Dumusque et al. 2011).

HD 77110 (*N*_{mes} = 16): this star shows a tentative very low-amplitude drift in radial velocity (amplitude ~ 1 m/s/yr). Such trend is not discussed in the literature, although to our knowledge this star has not been included in any other high-precision radial-velocity survey. No significant periodic signal is found in the data.

HD 78747 (*N*_{mes} = 26): the analysis of the generalized Lomb Scargle periodogram (Table 8) suggests the presence of a 3.1 day period signal in the data. It is indeed possible to find a satisfactory Keplerian fit with this period, an amplitude of 2.0 m s⁻¹, and eccentricity of 0.26. In order to confirm this signal we obtained a series of 14 new radial velocities from April to July 2010. The analysis of the data (to be published in a separate paper) does not reveal any 3-day signal.

HD 79601 (*N*_{mes} = 16): this is another case of low-amplitude drift (-0.6 m/s/yr), whose cause is not identified. No significant periodic signal was found in the data, even after subtracting the linear drift. No reference for a possible companion was found in the literature.

HD 88725 (*N*_{mes} = 22): the radial velocity measurements of this star present a low amplitude linear trend (-1.9 m/s/yr). The analysis of the residuals of a linear fit to the data show the presence of a peak around 3 days. However, the FAP of this peak suggests that it is not significant. The small number of measurements precludes any further conclusions. No planet was found around this star in other high precision planet search surveys (e.g. Fischer & Valenti 2005).

HD 109310 (*N*_{mes} = 15): a low-amplitude drift is suggested from our radial velocity data (-1.5 m/s/yr). The residuals of a

linear fit to the data show an rms of ~ 2.5 m s⁻¹, still above the average radial velocity error of 1.6 m s⁻¹. A frequency analysis of the residuals does not reveal, however, any significant signal. Having so few measurements does not allow us to make any further conclusions about this case.

HD 113679 (*N*_{mes} = 6): a long-term and low-amplitude (~ 1.7 m s⁻¹) linear trend is observed for this star over a span of ~ 1500 days. The reduced number of data points obtained does not allow reaching any firm conclusions about the observed variation. We found no reference in the literature to any variability (e.g. Nordström et al. 2004), although this star was not included (to our knowledge) in any other high-precision radial-velocity survey.

HD 124785 (*N*_{mes} = 17): this star presents a clear excess rms in the radial velocities, when compared to the average error. As for HD 59984, however, the atmospheric parameters derived by Sousa et al. ($T_{\text{eff}} = 5867$ K, $\log g = 4.20$) suggest that this star has already evolved off the main sequence. This may explain the excess power observed, and is supported by not finding any significant periodicity in the data.

HD 148211 (*N*_{mes} = 31): the statistical tests done above suggest there is a significant drift with a very small amplitude (-0.6 m s⁻¹). This signal is visually very marginal, though. No significant periodicity is found in the data. Our statistical tests also do not indicate any significant radial-velocity excess.

HD 150177 (*N*_{mes} = 30): a high level of residuals is seen in the data for this star. No significant periodic signal(s) was found though. The early spectral type and evolutionary status suggested by the precise atmospheric parameters derived by Sousa et al. ($T_{\text{eff}} = 6216$ K, $\log g = 4.18$) indicate that the

Table 7. Variability tests for stars with at least 6 measurements (HD numbers above 100 000).

Name	N	σ_i [m s ⁻¹]	σ_e [m s ⁻¹]	$P(F)$	χ^2_{constant}	$P(\chi^2_{\text{constant}})$	Slope [m/s/yr]	χ^2_{slope}	$P(F_{\text{slope}})$	FAP
HD 102200	7	5.4	8.1	0.279	7.7	0.260	0.835	4.5	0.127	0.023
HD 104800	6	1.8	1.5	0.795	3.2	0.663	-0.677	2.1	0.325	0.129
HD 107094	14	1.8	599	<10⁻⁹	$1.8 \times 10^{+6}$	<10⁻⁹	429.034	$1.3 \times 10^{+4}$	<10⁻⁹	<1/720
HD 108564	6	1.6	1.3	0.791	3.8	0.573	-0.436	2.5	0.321	0.176
HD 109310	15	1.6	3.7	0.003	78.5	<10⁻⁹	-1.460	47.9	3.1×10^{-4}	0.003
HD 109684	6	1.9	2.5	0.450	8.0	0.158	-0.202	6.3	0.645	0.170
HD 111777	6	1.5	1.2	0.814	4.2	0.522	-0.355	2.9	0.403	0.299
HD 113679	6	2.2	2.7	0.496	9.8	0.082	1.697	0.4	1.7×10^{-4}	<1/720
HD 123517	9	3.1	49.5	<10⁻⁹	2039	<10⁻⁹	34.103	3.2	<10⁻⁹	<1/720
HD 124785	17	2.2	4.7	0.004	78.8	<10⁻⁹	-1.794	68.3	0.080	0.100
HD 126681	13	2.4	3.7	0.116	23.6	0.023	-0.788	20.1	0.201	0.057
HD 126793	7	2.3	4.1	0.169	14.1	0.029	0.737	7.7	0.100	0.020
HD 126803	7	2.6	4.8	0.143	12.9	0.044	0.414	8.7	0.252	0.022
HD 134440	10	2.4	2.5	0.562	9.7	0.375	-0.171	9.0	0.857	0.083
HD 144589	11	4.0	34.7	<10⁻⁹	604	<10⁻⁹	25.404	14.2	<10⁻⁹	0.001
HD 148211	31	1.6	2.5	0.011	76.0	7.0×10^{-6}	-0.600	67.8	8.2×10^{-4}	0.006
HD 148816	6	1.6	1.8	0.569	5.7	0.341	0.198	3.6	0.305	0.070
HD 149747	9	4.7	4.6	0.666	10.4	0.237	-0.904	7.9	0.213	0.142
HD 150177	30	1.6	4.8	<10⁻⁹	327	<10⁻⁹	-0.091	326	1.000	0.313
HD 167300	9	1.8	2.1	0.479	12.4	0.132	-0.135	11.9	0.968	0.596
HD 171028	48	1.5	33.8	<10⁻⁹	$2.9 \times 10^{+4}$	<10⁻⁹	8.624	$2.7 \times 10^{+4}$	1.0×10^{-6}	0.208
HD 171587	14	1.3	6.0	2.0×10^{-6}	261	<10⁻⁹	1.791	225	0.185	0.175
HD 175607	7	1.7	1.2	0.897	4.4	0.618	1.082	1.5	0.015	0.051
HD 181720	29	1.8	6.3	<10⁻⁹	617	<10⁻⁹	-0.899	587	0.247	0.107
HD 190984	46	2.3	39.1	<10⁻⁹	$2.0 \times 10^{+4}$	<10⁻⁹	20.284	2910	<10⁻⁹	<1/720
HD 197083	12	1.6	2.7	0.080	45.1	5.0×10^{-6}	1.517	30.8	0.016	0.278
HD 197197	21	1.7	2.9	0.022	49.0	3.1×10^{-4}	-0.609	46.9	0.721	0.061
HD 199288	14	1.0	1.0	0.509	15.7	0.264	-0.373	11.4	0.009	0.064
HD 199604	6	1.8	1.8	0.707	3.6	0.610	2.391	1.2	0.041	0.055
HD 199847	7	2.0	2.9	0.331	9.3	0.156	1.331	4.5	0.059	0.021
HD 206998	6	2.5	2.8	0.563	5.7	0.332	-1.071	2.0	0.047	0.018
HD 207869	17	1.4	1.4	0.613	19.1	0.266	-0.305	17.4	0.339	0.373
HD 210752	17	1.4	2.1	0.104	39.0	0.001	0.378	34.3	0.126	0.039
HD 215257	37	1.6	14.4	<10⁻⁹	1870	<10⁻⁹	-15.045	343	<10⁻⁹	<1/720
HD 218504	15	1.3	2.0	0.122	30.6	0.006	-0.449	26.4	0.140	0.095
HD 224817	30	1.4	3.4	6.0×10^{-6}	109	<10⁻⁹	-0.134	105	0.691	0.090

observed noise may be due to stellar oscillation and granulation phenomena.

HD 171587 ($N_{\text{mes}} = 14$): the radial velocity measurements of this star show a clear radial-velocity rms excess with respect to the measurement errors. The analysis of the data show that, excluding the point at JD = 54 638 ($\sim 20 \text{ m s}^{-1}$ above the average of the other measurements), a clear periodic signal appears that is best fit with a Keplerian function with $P = 4.49$ days, $K = 4.0 \text{ m s}^{-1}$, and $e = 0.57$. The residuals of this fit are only 0.56 m s^{-1} (compared to the average error of 1.3 m s^{-1}), making us suspect that there are not enough points to obtain a reliable fit. This signal would be compatible with the presence of a 7.1 Earth mass planet orbiting this $0.76 M_{\odot}$ star ($T_{\text{eff}} = 5412 \text{ K}$, $\log g = 4.59$, $[\text{Fe}/\text{H}] = -0.64$). The analysis of the Ca II H and K lines suggests that this star is chromospherically very active ($\log R'_{\text{HK}} = -4.75$). Interestingly, this activity value indicates a rotational period of 21 days (Noyes et al. 1984), ~ 5 times longer than the observed signal. A periodogram of the individual S_{MW} values shows a peak around 23.5 days, with a significance level of 93%. This peak may be the signature of the rotational period of the star. We note, however, that the Keplerian fit described is only based on 13 points (excluding the above-mentioned date), and the time sampling is very wide (individual points are very

separated in time). A series of additional data points were obtained in 5 consecutive nights in July 2010 under ESO program 085.C-0063 (to be published in a separate paper). The results do not show any clear 4.5 day periodicity.

HD 224817 ($N_{\text{mes}} = 30$): according to our statistical tests, this star shows an rms above the expected value when taking the average internal errors into account. However, this is largely due to the only point at JD = 53 289, without which no significant variation is seen.

5.3.1. Previously announced planets

Three stars in our sample were previously announced as harboring long-period giant planets (Santos et al. 2007, 2010), see Fig. 7. For one of these, new HARPS radial velocities were obtained after the discovery paper.

HD 171028: this star was the first in our sample to be announced to have an orbiting giant planet (Santos et al. 2007). Since the announcement paper, 29 new radial velocity measurements were obtained (in a total of 48), allowing us to put stronger constraints to the orbital parameters of HD 171028b: period of 550 days, eccentricity of 0.59, and minimum mass of $1.98 M_{\text{Jup}}$ (supposing a stellar mass of $1.01 M_{\odot}$ – Sousa et al. 2011). In

Table 8. Periodogram variability tests for stars with at least 12 measurements.

Star [†]	FAP [%]	Period [days]	Amplitude [m s ⁻¹]
CD-2310879	1.08	4.63	14.2
HD 967	41.09	2.48	1.3
HD 11397 ^d	91.19	2.50	1.2
HD 17865	22.16	4.30	1.8
HD 22879	7.53	6.11	1.4
HD 31128	29.77	16.81	4.0
HD 40865	76.46	8.69	1.3
HD 51754	91.65	18.96	1.6
HD 56274 ^d	90.40	4.78	1.9
HD 59984	3.80	10.08	2.5
HD 75745	28.95	307.83	3.0
HD 77110 ^d	92.28	7.06	1.4
HD 78747	0.94	3.09	1.7
HD 79601 ^d	38.62	9.56	1.1
HD 88725 _d	54.37	3.44	1.5
HD 107094 ^d	<10 ⁻⁴	1898.28	80.3
HD 109310 ^d	5.93	77.34	6.0
HD 124785	55.12	41.84	6.6
HD 126681	17.71	1034.04	6.2
HD 148211	53.78	63.39	1.9
HD 150177	2.46	147.62	5.6
HD 171028	<10 ⁻⁴	500.55	47.1
HD 171028 ^p	3.81	16.71	2.3
HD 171587	71.19	4.30	5.1
HD 181720	<10 ⁻⁴	973.47	8.9
HD 181720 ^p	50.68	56.25	1.3
HD 190984	<10 ⁻⁴	1948.73	61.6
HD 190984 ^p	36.50	33.29	3.1
HD 197083	21.06	87.60	7.1
HD 197197	9.67	5.36	2.8
HD 199288	77.67	59.37	2.0
HD 207869	26.90	15.67	2.5
HD 210752	25.38	2.60	1.9
HD 215257 ^d	20.28	8.05	3.7
HD 218504	80.32	4.96	1.9
HD 224817	8.62	9.15	2.0

Notes. ^(†) Names with suffix *d* and *p* denote the results after subtraction of the linear drift and Keplerian solutions, respectively.

Table 9 we present our solution. A Lomb Scargle Periodogram of the residuals reveal the presence of a non significant peak at ~ 17 day period. This may be related to the rotational period of the star. We tried to fit a Keplerian function to the residuals of the Keplerian fit, but no satisfactory solution was found.

HD 181720 and *HD 190984*: giant planets were found around these two stars and recently announced in Santos et al. (2010). The orbital parameters for the two planets are listed in Table 9. We refer to the discovery paper for more details.

5.3.2. High-amplitude linear drifts

A few stars in our sample present very clear long-term trends with total amplitudes of at least 10 to 20 m s⁻¹. These are compatible with the existence of long period giant planets or brown dwarfs. However, the insufficient time coverage of the data does not allow making any conclusion about the origin of the observed signal.

HD 11397: the 33 radial velocities of this star show the signature of a clear long-term trend with a total amplitude of

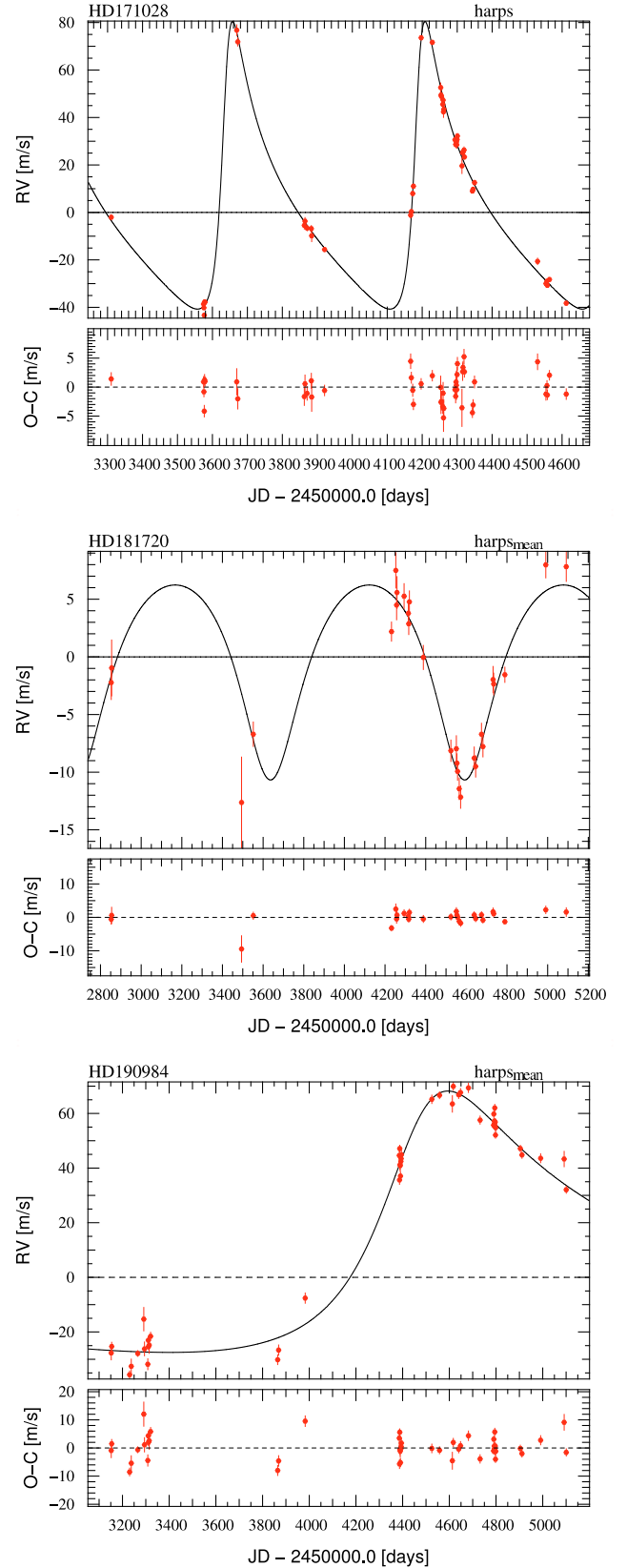


Fig. 7. Radial velocity time series for the 3 stars with planets discussed in Sect. 5.3.1.

33 m s⁻¹ over 2075 days. When excluding the first two measurements, the trend shows a slight curvature. The data could be well fit by a linear slope, together with a low-amplitude long-period

Table 9. Elements of the fitted orbits for known planets.

	HD 171028	HD 181720 [†]	HD 190984	
P	550 ± 3	956 ± 14	4885 ± 1600	[d]
T	$2\,454\,187 \pm 1$	$2\,453\,631 \pm 30$	$2\,449\,572 \pm 1600$	[d]
a	1.32	1.78	5.5	[AU]
e	0.59 ± 0.01	0.26 ± 0.06	0.57 ± 0.10	
V_r	13.641 ± 0.001	-45.3352 ± 0.0004	20.269 ± 0.004	[km s ⁻¹]
ω	304 ± 1	177 ± 12	318 ± 5	[deg]
K_1	60.6 ± 1.0	8.4 ± 0.4	48 ± 1	[m s ⁻¹]
$f_1(m)$	6.61×10^{-9}	0.053×10^{-9}	30.95	[M_\odot]
$\sigma(\text{O-C})$	2.3	1.37	3.44	[m s ⁻¹]
N	48	28	47	
$m_2 \sin i$	1.98	0.37	3.1	[M_{Jup}]

Notes. ^(†) Orbital parameters from Santos et al. (2010).

signal. However, the lower quality of the first two data points (photon noise error of 2–4 m s⁻¹ and obtained with short exposure times not allowing suppression of stellar oscillation noise) keeps us from deeper insight into the observed signal. No significant short-period signal is found in the data. A quadratic fit that excludes the first two points shows a low rms of 1.27 m s⁻¹, not strongly above the average photon noise (0.90 m s⁻¹). More data are needed to clarify this case.

HD 123517: the 9 radial velocity measurements of this star reveal a clear long-term linear drift (~ 150 m s⁻¹ over ~ 1600 days). The residuals of a linear fit to the data (1.5 m s⁻¹) are smaller than the average photon noise error of the measurements (2.3 m s⁻¹; this is one of the faintest stars in our sample with $m_v = 9.6$), suggesting that no detectable short period signal is hidden in the data. More data are needed to confirm the source of the observed radial velocity variation.

HD 144589: we obtained 11 radial velocity measurements of this star, spanning a total of ~ 1500 days. The data shows the presence of a clear linear trend, with a fitted slope of 25 m s⁻¹ yr⁻¹. The residuals of a linear fit to the data (4.0 m s⁻¹) are slightly above the average photon noise of the measurements (3.4 m s⁻¹). The stellar atmospheric parameters derived for this star ($T_{\text{eff}} = 6372$ K, $\log g = 4.28$, $[\text{Fe}/\text{H}] = -0.05$) by Sousa et al. (2011) suggest that this is one of the hottest stars in our sample and likely slightly evolved off the main sequence. Stellar oscillations, along with the relatively high projected rotational velocity (5.6 km s⁻¹ – derived from the HARPS cross-correlation function), may explain the excess observed scatter.

HD 215257: the 37 radial velocities of this star (average error of 1.6 m s⁻¹) indicate the presence of a low amplitude linear drift (-15 m s⁻¹ yr⁻¹ over 1700 days). A signal with a similar slope was also found by Sozzetti et al. (2009) using lower precision data from their Keck-HIRES survey. The high residuals (3.98 m s⁻¹) around the linear trend indicate an extra signal in the data. No reliable Keplerian fit was found, though, and no significant peak is found in a generalized Lomb Scargle periodogram. Since the star is an early-G/late-F dwarf with $T_{\text{eff}} = 6052$ K, $\log g = 4.46$, and $[\text{Fe}/\text{H}] = -0.63$ (Sousa et al. 2011), at least part of this signal may come from stellar oscillation and granulation “noise” (more important in early type stars – Mayor et al. 2003; Dumusque et al. 2011). More data are needed to confirm that this is the only source of the observed rms.

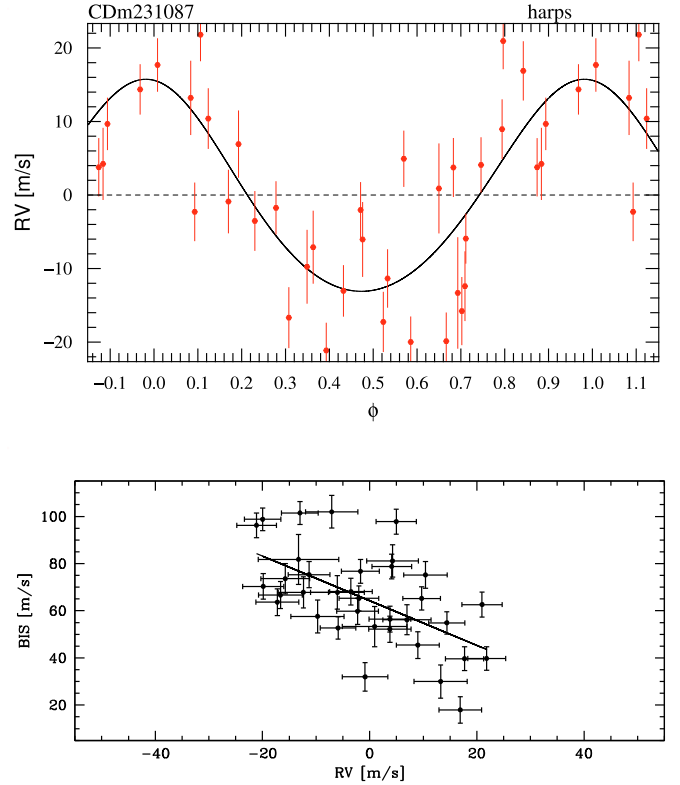


Fig. 8. Top: phase folded radial-velocity measurements of CD-2310879 with a period of 4.626 days. The line represents the best Keplerian function fit. Bottom: radial velocities as a function of the HARPS cross-correlation bisector inverse slope. The line represents a linear fit to the data.

5.3.3. Activity-induced periodic signals

CD-2310879: the 35 radial-velocity measurements of this F dwarf ($T_{\text{eff}} = 6788$ K, $\log g = 4.67$, $[\text{Fe}/\text{H}] = -0.24$) present an rms of 12.9 m s⁻¹, clearly above the median photon noise (3.9 m s⁻¹). A Lomb Scargle periodogram shows a significant peak around 4.5 days, well fit by a Keplerian function (see Fig. 8) with $P = 4.626$ days, eccentricity of 0.092, and semi-amplitude of 14.4 m s⁻¹ (residuals of 3.96 m s⁻¹, similar to the photon

noise). This signal is compatible with the existence of a planet with 42 times the mass of the Earth orbiting this $1.20 M_{\odot}$ star. However, a Lomb Scargle periodogram of the bisector inverse slope (BIS) of the HARPS cross-correlation function shows a similar peak at ~ 4.5 days. A clear negative correlation is also seen between BIS and the radial velocities (slope = -0.94 ± 0.23 – Fig. 8), typical of the signal expected from activity-induced radial-velocity variations (see case of HD 166435 – Queloz et al. 2000). The high value of the activity index obtained from the HARPS spectra, $\log R'_{HK} = -4.60$, suggests a rotational period around 4 days, similar to the observed radial-velocity periodicity (Noyes et al. 1984). We thus conclude that the best explanation for the observed radial-velocity variation of this star is given by active regions modulated by stellar rotation.

5.3.4. Ambiguous cases: new candidate planets

HD 107094: a total of 14 radial velocities were obtained for this star, showing a clear long-term (quasi-linear) radial-velocity signal. Twelve of these measurements were obtained within the HARPS GTO program, and a last two in July 2010 under ESO program 085.C-0063. In a first analysis, the total amplitude ($\sim 2.5 \text{ km s}^{-1}$ over 2355 days) suggests there is a stellar or sub-stellar companion orbiting this 0.8 solar mass star. A single Keplerian fit to the data shows that it is well fit by a long-period Keplerian function, though the orbital parameters are difficult to constrain (see Fig. 9). The residuals of this fit, on the order of 2.1 m s^{-1} , are still high, and they called attention to a different possible orbital solution to the system. Indeed, a fit of the linear drift together with a Keplerian function reveals the presence of a possible shorter period solution, with $P \sim 1870$ days, $K = 88 \text{ m s}^{-1}$, and $e = 0.13$ (Table 10). This signal, first detected using only the GTO data, is compatible with the presence of a 4.5 Jupiter mass companion. The residuals of this fit (1.10 m s^{-1}) are significantly better than in the previous case. The fitted linear trend (which, to our knowledge, has not been previously reported in the literature) has a slope of $402 \pm 1 \text{ m/s/yr}$. More data are now needed to disentangle the two possible solutions, but we are likely seeing a new giant planet. Interestingly, with $[\text{Fe}/\text{H}] = -0.51$ (Sousa et al. 2011), HD 107094 is close to the high-metallicity limit of our sample.

HD 197083: although the statistical analysis done for this star does not indicate any strong signal, a visual inspection of the radial velocities hints at the presence of a long-term periodic signal ($P \sim 1500\text{--}2000$ days), see Fig. 6. The number of points covering the first ~ 1000 days is very reduced (3) with high error bars. More data are thus clearly needed to confirm this signal.

6. Discussion and conclusions

In this paper we present the overall results of our HARPS program to search for planets orbiting a sample of metal-poor stars. In a total of 104 stars, 3 giant planets were confirmed, and one more very promising giant planet candidate is presented. These discoveries significantly increase the number of known giant planets orbiting metal-poor stars (see also case of HD 155358 – Cochran et al. 2007). Several binary stars were also found in the sample.

A proper statistical analysis of our results requires not only identifying the planetary signals in our time series but also assessing their detection limit; i.e. what planets, as a function of mass and period, can be rejected considering our observations. Although this is the topic of a forthcoming paper, partial figures can already be given. Excluding the 16 stars discussed in

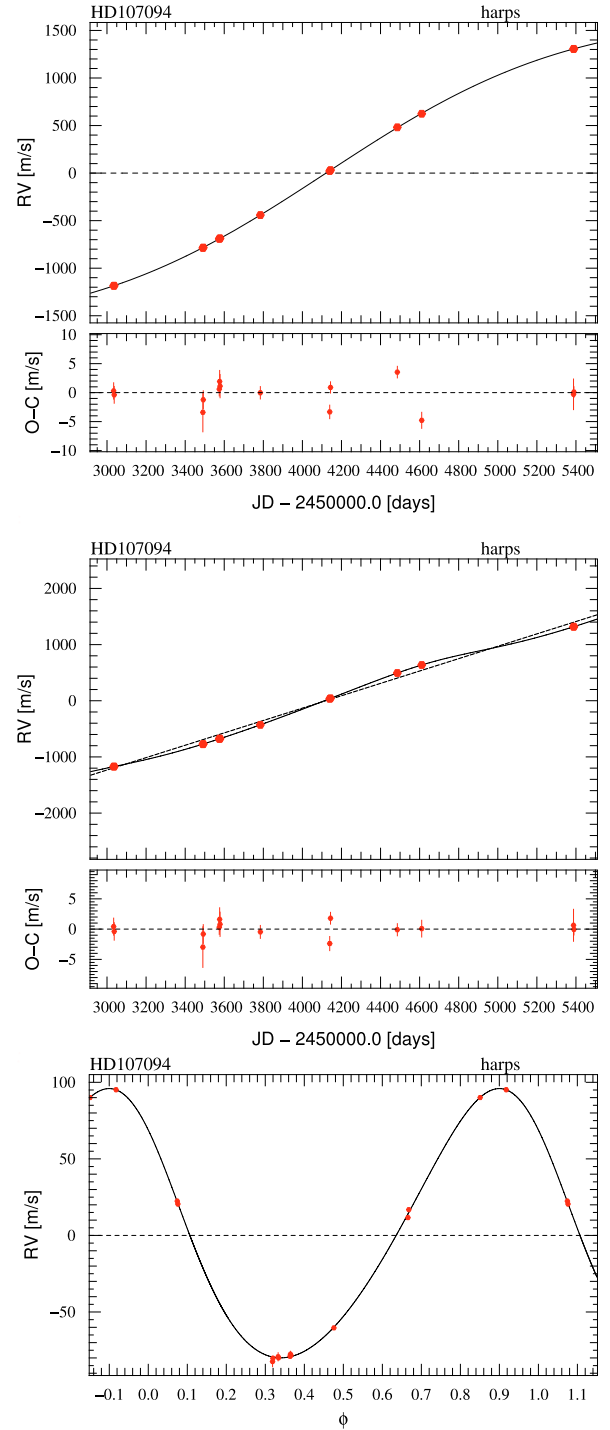


Fig. 9. *Top:* radial velocity measurements of HD 107094 and best 1-Keplerian fit to the data. *Middle:* same as above but after fitting a linear trend, together with a Keplerian function. In both cases the residuals are shown. *Bottom:* phase-folded radial velocity measurements with the period of the candidate planet.

Sect. 4 (targets not suitable for a high-precision radial-velocity planet search), our sample is constituted of 64/87 stars with at least 6/3 radial velocity measurements. We have detected at least 3 giant planets with masses greater than 0.3 Jupiter masses and with periods ranging from a few hundred to a few thousand days. Of course, time series with only a few measurements ($\sim 3\text{--}6$) cannot always rule out a Jupiter-mass companion on a short or

Table 10. Elements of the fitted orbit for HD 107094.

P	1870 ± 34	[d]
T	$2\,454\,765 \pm 29$	[d]
a	2.76	[AU]
e	0.13 ± 0.02	
V_r	15.33 ± 0.05	[km s ⁻¹]
ω	46 ± 3	[deg]
K_1	88 ± 5	[m s ⁻¹]
$f_1(m)$	128.3×10^{-9}	[M_\odot]
$\sigma(\text{O-C})$	1.10	[m s ⁻¹]
N	14	
$m_2 \sin i$	4.5	[M_{Jup}]

moderate period orbit. Moreover, we have a possible fourth detection and several more stars with a linear RV drift indicative of a long-period companion. Three (3) detections over 87 targets, or $3.4^{+3.2}_{-1.0}\%$, is therefore a lower estimate to the frequency of Jupiter-mass planets orbiting metal-poor stars. If we only consider stars with [Fe/H] between -0.40 and -0.60 dex (an interval where the stars with planets are in our sample), then only 34 stars with at least 3 measurements exist, and the percentages increase to $11.3^{+4.9}_{-5.3}\%$.

We can additionally note that no planet has been detected around the 32 stars with [Fe/H] < -0.60 dex and at least 6 measurements. For these stars it is reasonable to assume completeness for Jupiter-mass planets on short or moderate period orbits (< 100 days). Those stars have metallicities from -1.4 to -0.6 dex, with a median value of -0.69 dex. A null detection for that subsample implies a maximum occurrence of Jupiter-mass planets (on short or moderate orbital periods) of $\sim 5\%$.

Santos et al. (2001, 2004b) have shown that the frequency of giant planets orbiting solar type dwarfs is a strong function of the stellar metallicity. This trend, confirmed by several other studies (e.g. Fischer & Valenti 2005; Johnson et al. 2010), makes these facts surprising. The above studies have also shown that the frequency of giant planets orbiting stars with metallicity near -0.5 dex is $\sim 3\%$ (see also review by Udry & Santos 2007), strongly below the $\sim 11\%$ mentioned above (though both results are still likely compatible within the error bars). We have to take into account, however, that the exquisite precision of HARPS has increased the planet detection rate when compared to the results of the lower precision programs on which the existence of the metallicity-giant planet correlation has been based (Santos et al. 2004b; Fischer & Valenti 2005). The present results, although based on small number statistics, may hint at a much higher frequency of giant planets around solar type stars (of all metallicities).

The stars with giant planets discovered in our survey (HD 171028, HD 181720, HD 190984, and likely HD 107094), all have metallicity values on the high-metallicity side of our sample (-0.48 , -0.53 , -0.49 , and -0.51 , respectively), see Fig. 1. This suggests that even for metal-poor stars the frequency of giant planets is a rising function of the stellar metallicity, a result that does not confirm former suspicions that the metallicity-giant planet correlation could be flat for [Fe/H] values below solar (Santos et al. 2004b). This result further suggests that the core accretion model of planet formation is still at play in these low metallicity values (Ida & Lin 2004b; Mordasini et al. 2009a). Since no planets were discovered in our sample at [Fe/H] significantly below -0.5 dex, and only one giant planet was found around a stars with lower metallicity (-0.68 dex – Cochran et al.

2007), this could also hint that we are close to the metallicity limit below which no giant planets can be formed. More data are, however, needed to settle this issue.

As mentioned in Sect. 2, it is interesting to observe that two of the stars discussed in Sect. 5.3.2, the ones that present long-term radial-velocity linear drifts (HD 123517 and HD 144589), have the highest metallicity values ($+0.09$ and -0.05 dex) among all the objects in our sample (see also Fig. 1). Both present relatively low-amplitude linear trends, suggestive of the presence of long-period giant planets. If such detections are confirmed, this result would be in line with the metallicity-giant planet correlation.

Interestingly, no short period planet was found in our data. All the 3 (or 4) giant planets discovered orbit in long-period orbits. This suggests that giant planets in short-period orbits are not common around stars with low metallicity, in agreement with the results of Sozzetti et al. (2009). The lack of such detections is, however, expected, since the frequency of hot jupiters in radial velocity surveys is only $\sim 1\%$ (Udry & Santos 2007). Only 87 stars were effectively monitored in the present survey, precluding a significant statistical meaning for this lack of detection.

Theoretical studies (e.g. Mordasini et al. 2009a), backed up by recent observations (e.g. Sousa et al. 2008), suggest that the frequency of low-mass planets may increase for stars in the metallicity range of our sample when compared to solar metallicity objects. That no Neptune or super-Earth mass planet has been discovered up to now in our sample does not contradict this conclusion. Instead, the observing strategy used (data sampling and exposure times) was simply not adequate for the purpose of finding such low-mass objects. A program with HARPS is presently being done to fill this gap.

Acknowledgements. We would like to thank the referee, Michael Endl, for the positive and constructive report. We acknowledge the support by the European Research Council/European Community under the FP7 through Starting Grant agreement number 239953. N.C.S. also acknowledges the support from Fundação para a Ciência e a Tecnologia (FCT) through program Ciência 2007 funded by FCT/MCTES (Portugal) and POPH/FSE (EC), and in the form of grants reference PTDC/CTE-AST/098528/2008 and PTDC/CTE-AST/098604/2008. SGS is supported by grant SFRH/BPD/47611/2008 from FCT/MCTES.

References

- Bonfils, X., Forveille, T., Delfosse, X., et al. 2005, *A&A*, 443, L15
- Bonfils, X., Delfosse, X., Udry, S., et al. 2010, *A&A*, submitted
- Boss, A. P. 1997, *Science*, 276, 1836
- Boss, A. P. 2002, *ApJ*, 567, L149
- Boss, A. P. 2006, *ApJ*, 644, L79
- Bouchy, F., Bazot, M., Santos, N. C., Vauclair, S., & Sosnowska, D. 2005, *A&A*, 440, 609
- Christensen-Dalsgaard, J. 2004, *Sol. Phys.*, 220, 137
- Cochran, D. C., Endl, M., Wittenmyer, R. A., & Bean, J. L. 2007, *ApJ*, in press
- Cumming, A., Marcy, G. W., & Butler, R. P. 1999, *ApJ*, 526, 890
- Da Silva, R., Udry, S., Bouchy, F., et al. 2006, *A&A*, 446, 717
- Dumusque, X., Udry, S., Lovis, C., Santos, N., & Monteiro, M. 2011, *A&A*, 525, A140
- ESA 1997, *The Hipparcos and Tycho Catalogues*
- Fischer, D. A., Laughlin, G., Butler, P., et al. 2005, *ApJ*, 620, 481
- Fischer, D. A., & Valenti, J. 2005, *ApJ*, 622, 1102
- Gonzalez, G. 1997, *MNRAS*, 285, 403
- Gratton, R. G., Sneden, C., Carretta, E., & Bragaglia, A. 2000, *A&A*, 354, 169
- Ida, S., & Lin, D. N. C. 2004a, *ApJ*, 604, 388
- Ida, S., & Lin, D. N. C. 2004b, *ApJ*, 616, 567
- Johnson, J. A., Butler, R. P., Marcy, G. W., et al. 2007, *ApJ*, 670, 833
- Johnson, J. A., Aller, K. M., Howard, A. W., & Crepp, J. R. 2010, *PASP*, 122, 905
- Latham, D. W., Stefanik, R. P., Torres, G., et al. 2002, *AJ*, 124, 1144
- Laughlin, G., Bodenheimer, P., & Adams, F. C. 2004, *ApJ*, 612, L73

⁴ The 1-sigma error bars were obtained using a binomial distribution.

- Lovis, C., & Mayor, M. 2007, *A&A*, 472, 657
- Lovis, C., Mayor, M., Pepe, F., et al. 2006, *Nature*, 441, 305
- Matsuo, T., Shibai, H., Ootsubo, T., & Tamura, M. 2007, *ApJ*, 662, 1282
- Mayer, L., Quinn, T., Wadsley, J., & Stadel, J. 2002, *Science*, 298, 1756
- Mayor, M., Pepe, F., Queloz, D., et al. 2003, *The Messenger*, 114, 20
- Mayor, M., Bonfils, X., Forveille, T., et al. 2009, *A&A*, 507, 487
- Mordasini, C., Alibert, Y., & Benz, W. 2009a, *A&A*, 501, 1139
- Mordasini, C., Alibert, Y., Benz, W., & Naef, D. 2009b, *A&A*, 501, 1161
- Nordström, B., Mayor, M., Andersen, J., et al. 2004, *A&A*, 418, 989
- Noyes, R. W., Hartmann, L. W., Baliunas, S. L., Duncan, D. K., & Vaughan, A. H. 1984, *ApJ*, 279, 763
- Paulson, D. B., Saar, S. H., Cochran, W. D., & Hatzes, A. P. 2002, *AJ*, 124, 572
- Pollack, J., Hubickyj, O., Bodenheimer, P., et al. 1996, *Icarus*, 124, 62
- Pourbaix, D., Tokovinin, A. A., Batten, A. H., et al. 2004, *A&A*, 424, 727
- Queloz, D., Mayor, M., Weber, L., et al. 2000, *A&A*, 354, 99
- Saar, S. H., & Donahue, R. A. 1997, *ApJ*, 485, 319
- Santos, N. C., Mayor, M., Naef, D., et al. 2000, *A&A*, 361, 265
- Santos, N. C., Israelian, G., & Mayor, M. 2001, *A&A*, 373, 1019
- Santos, N. C., Mayor, M., Naef, D., et al. 2002, *A&A*, 392, 215
- Santos, N. C., Bouchy, F., Mayor, M., et al. 2004a, *A&A*, 426, L19
- Santos, N. C., Israelian, G., & Mayor, M. 2004b, *A&A*, 415, 1153
- Santos, N. C., Mayor, M., Bouchy, F., et al. 2007, *A&A*, 474, 647
- Santos, N. C., Mayor, M., Benz, W., et al. 2010, *A&A*, 512, A47
- Setiawan, J., Rodmann, J., da Silva, L., et al. 2005, *A&A*, 437, L31
- Sousa, S. G., Santos, N. C., Mayor, M., et al. 2008, *A&A*, 487, 373
- Sousa, S. G., Santos, N. C., Israelian, G., et al. 2011, *A&A*, 526, A99
- Sozzetti, A., Torres, G., Latham, D. W., et al. 2009, *ApJ*, 697, 544
- Tinney, C. G., Butler, R. P., Marcy, G. W., et al. 2003, *ApJ*, 587, 423
- Udry, S., & Santos, N. 2007, *ARAA*, 45, 397
- Zacharias, N., Monet, D. G., Levine, S. E., et al. 2004, in *BAAS*, 36, 1418
- Zechmeister, M., & Kürster, M. 2009, *A&A*, 496, 577
- Zechmeister, M., Kürster, M., & Endl, M. 2009, *A&A*, 505, 859